

Effect of developer molecular size on roughness of dissolution front in electron-beam resist

T. Yamaguchi and H. Namatsu

Citation: *J. Vac. Sci. Technol. B* **22**, 1037 (2004); doi: 10.1116/1.1736647

View online: <http://dx.doi.org/10.1116/1.1736647>

View Table of Contents: <http://avspublications.org/resource/1/JVTBD9/v22/i3>

Published by the AVS: Science & Technology of Materials, Interfaces, and Processing

Related Articles

Improved imaging properties of thin attenuated phase shift masks for extreme ultraviolet lithography

J. Vac. Sci. Technol. B **31**, 021606 (2013)

Fabrication of multiscale electrodes on organic photovoltaic thin films and in situ electrical characterization by nanostencil combined with Qplus AFM

J. Vac. Sci. Technol. B **31**, 021803 (2013)

Origin of defects on targets used to make extreme ultraviolet mask blanks

J. Vac. Sci. Technol. A **31**, 021403 (2013)

Benefits of plasma treatments on critical dimension control and line width roughness transfer during gate patterning

J. Vac. Sci. Technol. B **31**, 012205 (2013)

Design and fabrication of a metallic nanostamp using UV nanoimprinting and electroforming for replicating discrete track media with feature size of 35nm

J. Vac. Sci. Technol. B **31**, 011801 (2013)

Additional information on *J. Vac. Sci. Technol. B*

Journal Homepage: <http://avspublications.org/jvstb>

Journal Information: http://avspublications.org/jvstb/about/about_the_journal

Top downloads: http://avspublications.org/jvstb/top_20_most_downloaded

Information for Authors: http://avspublications.org/jvstb/authors/information_for_contributors

ADVERTISEMENT



www.raith.com

eLINE plus

- ▶ fabricate
- ▶ modify
- ▶ manipulate
- ▶ measure

Nanoengineering beyond Electron Beam Lithography

Raith
INNOVATIVE SOLUTIONS FOR NANOFABRICATION

Effect of developer molecular size on roughness of dissolution front in electron-beam resist

T. Yamaguchi^{a)} and H. Namatsu

NTT Basic Research Laboratories, NTT Corporation 3-1 Morinosato Wakamiya, Atsugi, Kanagawa 243-0198, Japan

(Received 23 January 2003; accepted 8 March 2004; published 4 May 2004)

This article describes the generation of roughness at the dissolution front of electron-beam positive-tone resist. The effect of a developer solvent molecule on the surface roughness as well as on the dissolution rate is investigated from the viewpoint of the size of a solvent molecule. The relationship between the dissolution rate and solvent molecular size is represented by two straight lines with different slopes in a homologous series of alkyl acetate solvents. A bending point, which corresponds to a critical molecular size, exists between ethyl and propyl acetate. This indicates that the dissolution behavior is largely different between acetates that are larger or smaller than the critical molecular size. The size of a solvent molecule is the dominant factor determining the degree of surface roughness. For a solvent molecule larger than the critical molecular size, the roughness becomes large because polymer aggregates appear on the dissolution front. For a smaller solvent molecule, on the other hand, no aggregates appeared and the dissolution front is flat and smooth. The critical molecular size is about the same as the average size of voids (free volume holes) in resist films. These results indicate that the roughness strongly depends on how a solvent molecule penetrates the resist film through void regions inhomogeneously distributed in the resist polymer matrix due to polymer aggregation. © 2004 American Vacuum Society.

[DOI: 10.1116/1.1736647]

I. INTRODUCTION

Future nanolithography will require the delineation of dense, very fine patterns less than 10-nm wide. At such small feature sizes, the line-edge roughness (LER) of resist patterns is a critical issue because it could degrade the resolution and linewidth accuracy.¹ It is essential to elucidate the origin of LER in order to find ways to reduce it. It is known that LER is related to factors involving the lithographic system, such as aerial image profiles,²⁻⁸ shot noise,^{9,10} and mask roughness,^{2,11} and also to resist materials and their development. Among these factors, resist materials and the development process are very important because they are surely the ultimate origin of LER. The LER of nonchemically amplified resists has been studied with regard to molecular weight, polydispersity, and the structure of base polymers,^{1,12} and by simulations of the development process.¹³ Though the relationship between these factors and LER were demonstrated, the origin of LER has not yet been definitely clarified. It is thought that LER is generated through inhomogeneous dissolution behavior at the nanometer scale. Therefore, an understanding of the mechanism by which the dissolution proceeds is necessary to elucidate its origin.

Polymer aggregates, which occur naturally in resist films,¹⁴⁻²⁰ are an important clue to this mechanism. Aggregates form even without prebaking or electron-beam exposure because they can clearly be observed in cross sections of resists films before prebaking. According to the model of aggregate extraction development,^{15,18,19} aggregates appear on the surface of exposed resist after development. This

model is based on the fact that the polymer density is slightly higher inside aggregates than outside them. That means that developer molecules can penetrate the regions surrounding the aggregates faster and dissolve them, with the result that aggregates appear on the surface. Once the surrounding polymers are completely dissolved, aggregates detach from the surface and float away, even if they themselves cannot be fully dissolved. Thus, the existence of polymer aggregates is strongly related to the dissolution process. This suggests that a further understanding of the behavior of the polymer aggregates during development is necessary for the elucidation of the origin of LER. Knowing how aggregates appear on the dissolution front during development will tell us how roughness is generated.

This article examines the relationship between the size of developer molecules and the roughness of the dissolution front in electron-beam positive-tone resist ZEP520. In addition, from the results of the dependence of the roughness of the dissolution front on the dissolution rate and exposure doses, we clarified that the size of developer solvent molecules is a dominant factor in the generation of roughness. We also discuss the origin of the roughness of the dissolution front in terms of polymer aggregate behavior through development.

II. EXPERIMENT

The resist used was a chain-scission-type positive-tone electron-beam resist ZEP520 (Nippon Zeon), which is a copolymer of methyl (α -chloroacrylate) and α -methylstyrene.²³ The resist was spin-coated on a wafer to a thickness of 500 nm and baked on a hot plate at 200 °C for 2 min. The resist

^{a)}Electronic mail: guchan@NTTBRL.jp

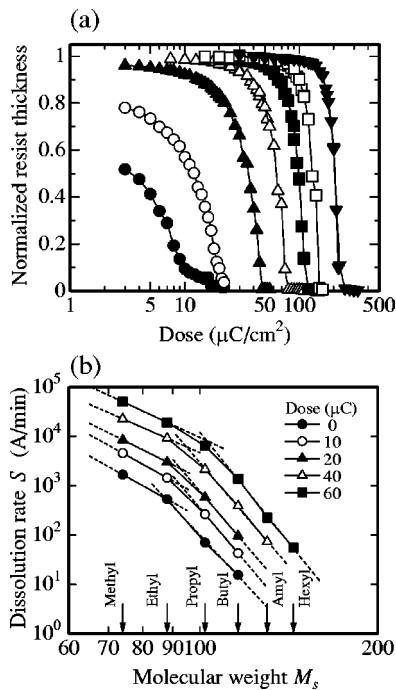


FIG. 1. (a) Contrast curves of ZEP520 films with a thickness of 500 nm for the seven *n*-alkyl-acetate developers: methyl-acetate (●), ethyl-acetate (○), propyl-acetate (▲), butyl-acetate (△), amyl-acetate (■), hexyl-acetate (□), and octyl-acetate (∇). Development time was 90 s except for methyl-acetate (60 s). (b) Dependence of the dissolution rate on the molecular weight of developer solvents for various exposure doses.

films were exposed to an electron beam with an acceleration voltage of 70 kV. The exposure area was 24 μm square. The exposed resist was then developed in various *n*-alkyl acetates at 23 °C for 5–150 s. All samples were rinsed in 2-propanol for 30 s after development. The remaining film thickness in exposed regions after development was measured with an interferometer (Nanospec 210XP, Nanometrics). The dissolution rate was obtained from a linear slope in the relationship between the amount of dissolution and development time. Observation of the morphology of the dissolution front was typified by that of the morphology of an exposed region after development. The surface morphology of exposed regions was observed with an atomic force microscope (AFM) (SPI3800/SPA500, Seiko Instruments) in the dynamic force mode. The scan area was 1 μm square (256 \times 256 pixels) for all samples. The magnitude of the surface roughness is defined as the root-mean-square (rms) value (1 σ) of the measured height in the AFM image.

III. RESULTS

A. Effect of molecular size of developer solvent on dissolution rate

The effect of the molecular size of the developer solvent on the dissolution rate was investigated. A homologous series of *n*-alkyl acetate between methyl- and octyl-acetate was used to vary the size of developer solvent molecules.

Contrast curves of 500-nm-thick ZEP520 films after development with these solvents are shown in Fig. 1(a). As

clearly seen in the figure, the dose to clear decreases as the size of solvents becomes small. Moreover, solvent molecules smaller than propyl-acetate make the unexposed regions of resist films soluble.

Figure 1(b) shows the logarithmic plot of the dissolution rate versus the molecular weight of developer solvent for various exposure doses. The dissolution rate decreases as the molecular weight M_s increases. This means that the dissolution rate is related to the molecular size of developer. The relationship between these two quantities can be expressed empirically by $S = k(1/M_s)^{-\beta}$, where k and β are constants.^{25–28} As seen in the figure, the relationship can be represented by two straight lines with different slopes for the alkyl-acetate solvents. The exponent β jumped from about 6 to about 14 between ethyl- and propyl-acetate. This rapid change in the slope indicates that the dissolution behavior is largely different for acetates larger or smaller than the critical molecular size corresponding to the bending point. Moreover, it is also found that the critical molecular size gradually increases with increasing exposure doses. For example, the critical molecular size corresponds to ethyl-acetate for unexposed resist, but to propyl-acetate for the resist exposed at 60 $\mu\text{C}/\text{cm}^2$.

B. Effect of developer on surface roughness of exposed ZEP resists

The dependence of surface roughness on the size of developer molecules was investigated. Figure 2 shows the surface morphology of lightly exposed ZEP resists after development with a homologous series of *n*-alkyl-acetate. As shown in the figure, it is clear that surface morphology strongly depends on the kind of developer, or in other words, the size of the developer. For octyl-acetate, many aggregates appear on the surface due to aggregate extraction, as we have reported.¹⁵ For hexyl-acetate, which is our standard developer used to obtain a high resolution with ZEP resists,²⁴ many aggregates also appear. For amyl-acetate, this is similar to what happens with *n*-hexyl-acetate, except that there are fewer aggregates on the surface. For butyl- and propyl-acetate, large undulation appears instead of the aggregates. This undulation is larger than the size of the aggregates observed on samples developed with larger alkyl-acetates. More interesting is that hardly any aggregates or undulation can be observed for ethyl- and methyl-acetate, indicating that aggregate extraction development does not occur with these two acetates.

From these results, surface morphology can be divided to three types: (1) a very flat and smooth surface for methyl- and ethyl-acetate, (2) a rough surface with large undulation for propyl- and butyl-acetate, and (3) a rough surface with polymer aggregates 20–30 nm in size for amyl- to octyl-acetate.

The exposure dose dependence of surface morphology for typical developer solvents of the above three types are shown in Fig. 3. For ethyl-acetate, the surface remains very flat regardless of the exposure dose. For propyl-acetate, large

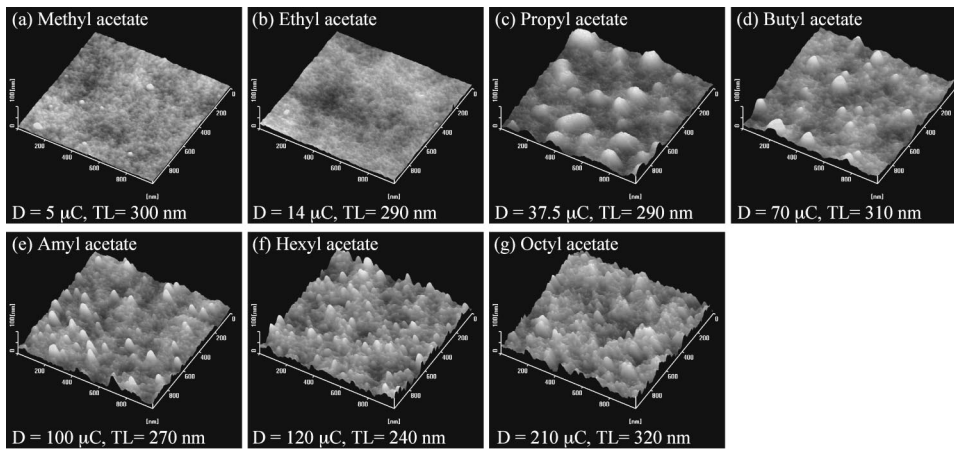


FIG. 2. AFM images of exposed regions of ZEP520 films with a thickness of 500 nm after development with the seven *n*-alkyl-acetate developers: methyl-acetate (●), ethyl-acetate (○), propyl-acetate (▲), butyl-acetate (△), amyl-acetate (■), hexyl-acetate (□), and octyl-acetate (▽). For comparison, AFM images of samples with the same thickness loss (TL) of about 300 nm are shown. Exposure dose (D) and TL are shown in each image.

undulation appears because the dissolution no longer proceeds uniformly even at low doses. With increasing dose, the number of undulations decreases and the surface becomes smoother. For butyl-acetate, the situation is the same as that for propyl-acetate, although the undulation is smaller. For amyl-acetate, the number of the aggregates decreases with increasing exposure doses. Although the surface morphology is quite different, a characteristic common to developers from propyl- to amyl-acetate is that the number of aggregates or undulations decreases as the exposure dose increases.

The dependence of surface roughness on exposure dose for various alkyl-acetates is summarized in Fig. 4. As expected from the surface morphology shown in Figs. 2 and 3, for methyl- and ethyl-acetate, the roughness is so small and remains almost constant, regardless of the exposure dose. For other acetates, the roughness increases rapidly until the thickness loss approaches 100–200 nm. This increase is attributed to the appearance of aggregates or large undulation on the surface, as shown in Figs. 2 and 3. For propyl- to hexyl-acetate, it is clear that the roughness gradually de-

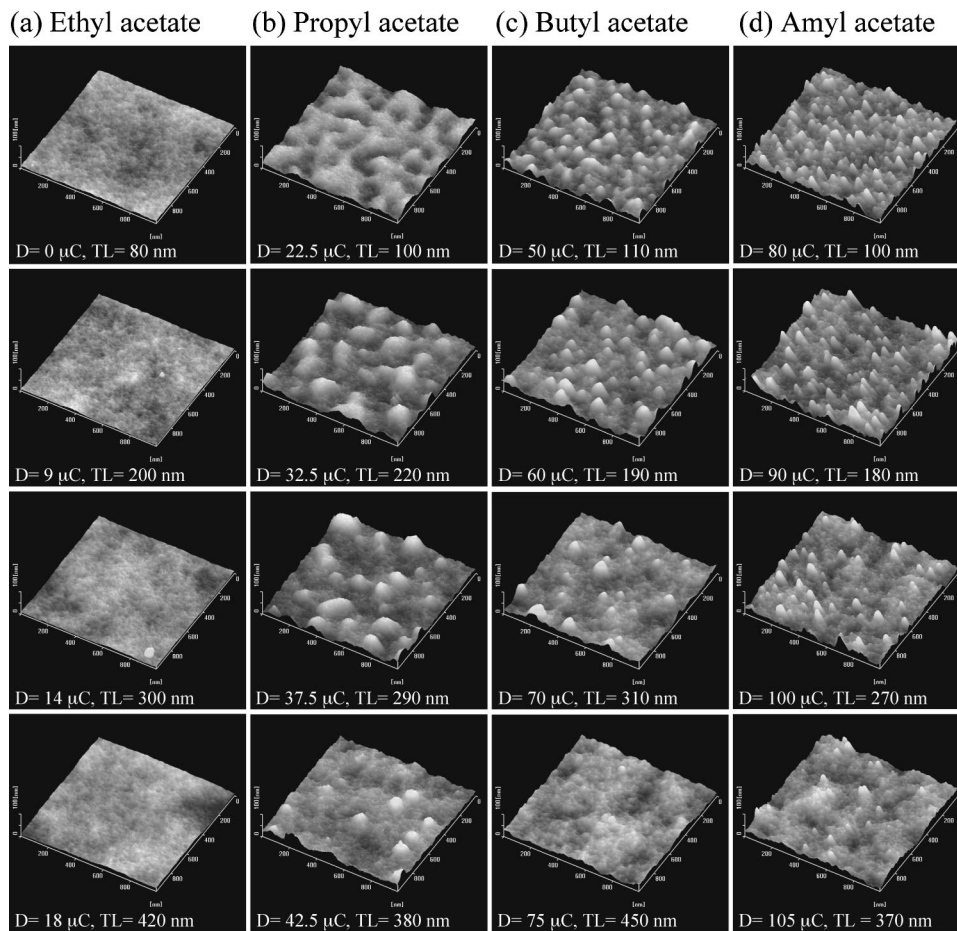


FIG. 3. AFM images of exposed regions of ZEP520 films with a thickness of 500 nm after development with four *n*-alkyl-acetate developers. Exposure dose (D) and TL are shown in each image.

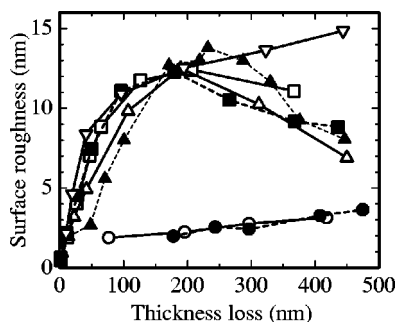


FIG. 4. Thickness loss dependence of surface roughness for various *n*-alkyl acetate developers: methyl-acetate (●), ethyl-acetate (○), propyl-acetate (▲), butyl-acetate (△), amyl-acetate (■), hexyl-acetate (□), and octyl-acetate (▽). Exposure dose was converted to thickness loss.

creases after the rapid increase. This decrease corresponds to the decrease in the number of undulations or aggregates on the surface. On the other hand, octyl-acetate tends to monotonically increase.

Figure 5 shows the thickness loss dependence of the correlation length (L_c) for samples developed with various acetates. The L_c , which corresponds to the average period of roughness, can be obtained by a scaling analysis.²⁰ It rapidly increases as thickness loss increases. As expected from the large undulation shown in Fig. 3, the L_c for propyl-acetate, whose value is over 100 nm, is much larger than that of the other acetates. This result is evidence that the critical molecular size is in between ethyl- and propyl-acetate for ZEP resist.

IV. DISCUSSION

A. Dissolution rate

In general, the solubility of a polymer strongly depends on its thermodynamic compatibility and on penetrability into the polymer matrix, which is related to the molecular size of the developer solvent.^{21,22}

First, we consider the thermodynamic compatibility. Thermodynamic compatibility is associated with interaction between the structural groups of the polymer and developer solvent. The three-dimensional solubility parameters^{21,22} are widely used for predicting the compatibility. The total solu-

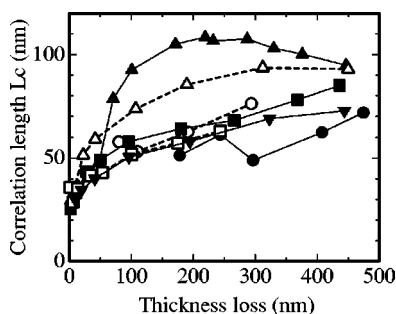


FIG. 5. Thickness loss dependence of the correlation length L_c for various *n*-alkyl-acetate developers: methyl-acetate (●), ethyl-acetate (○), propyl-acetate (▲), butyl-acetate (△), amyl-acetate (■), hexyl-acetate (□), octyl-acetate (▽). Exposure dose was converted to thickness loss.

TABLE I. Solubility parameters for a homologous series of *n*-alkyl acetate, monomer, and polymer.

Component	Solubility parameters [(MPa) ^{1/2}]			
	δ_D	δ_P	δ_H	δ_t
<i>Acetate</i>				
Methyl-acetate	15.50	7.20	7.60	18.70
Ethyl-acetate	15.80	5.30	7.20	18.15
Propyl-acetate	15.30	4.30	7.60	17.62
Butyl-acetate	15.80	3.70	6.30	17.41
Amyl-acetate	15.80	3.30	6.10	17.26
Hexyl-acetate	15.80	2.90	5.90	17.11
<i>Polymer</i>				
P(MMA-St) ^a	19.96	8.14	5.91	22.35
PMMA	18.64	10.52	7.51	22.68
PS	21.28	5.75	4.30	22.46
<i>Monomer</i>				
MMA-St ^a	17.20	3.75	4.75	18.20
(M α CA)-St ^a	17.25	4.15	6.30	18.83
MMA	15.80	6.50	5.40	17.90
M α CA	15.90	7.30	8.50	19.45
St	18.60	1.00	4.10	19.10
α MSt	17.40

^aEach solubility parameter of a compound is assumed to be the average value of each parameter of its component.

bility parameter, δ_t has three components: nonpolar (dispersion) δ_D ; polar (permanent dipole-dipole moment) δ_P ; and hydrogen bonding δ_H . Their relationship is $(\delta_t)^2 = (\delta_D)^2 + (\delta_P)^2 + (\delta_H)^2$. The degree of compatibility is characterized by the solubility parameter "distance" R_a between solvent and polymer coordinates in solubility parameter space: $(R_a)^2 = 4(\delta_{D2} - \delta_{D1})^2 + (\delta_{P2} - \delta_{P1})^2 + (\delta_{H2} - \delta_{H1})^2$, where 1 and 2 indicate solvent and polymer, respectively.²¹ The shorter the distance R_a is, the higher the compatibility between them becomes.

For an evaluation of the compatibility between the base polymer of ZEP resist and a homologous series of *n*-alkyl-acetate, their solubility parameters are needed. However, the solubility parameter of the base polymer of ZEP resist is unknown. We therefore use the average value of solubility parameters of poly(methylmethacrylate) (PMMA) and polystyrene (PSt) instead. This is because these structures are similar to the monomer components of the ZEP polymer, methyl(α -chloroacrylate) (M α CA) and α -methylstyrene (α MSt).

Solubility parameters of a homologous series of *n*-alkyl-acetate, polymers and their monomers are shown in Table I. For *n*-alkyl-acetate, the value of the polar component increases as the size of alkyl group in ester decreases. For polymers, the values of the polar and hydrogen bonding components are larger in PMMA than in PS, as would be expected from the existence of carboxyl group in PMMA. Each solubility parameter of copolymer P(MMA-St) is assumed to be the average of each value of PMMA and PSt. The difference in the solubility parameter between the copolymer P(MMA-St) and the ZEP polymer is expected from the difference of the solubility parameter of each monomer. The substitution of a chlorine atom for a methyl group in the

TABLE II. Distance Ra between polymer and a homologous series of *n*-alkyl acetate.

Component	Distance Ra		
	Ra(PMMA)	Ra(PS)	Ra[P(MMA-St)]
Methyl-acetate	7.104	12.11	9.128
Ethyl-acetate	7.721	11.35	8.885
Propyl-acetate	9.128	12.49	10.22
Butyl-acetate	8.958	11.33	9.437
Amyl-acetate	9.294	11.37	9.625
Hexyl-acetate	9.639	11.44	9.830

α -position of methacrylate leads to the increase of the polar and hydrogen-bonding components. The effect of the substitution of a methyl group for a hydrogen atom in the α -position of styrene is not clear because only the total solubility parameter of α MSt is known. However, it is obvious that the value of each component parameter of α -methylstyrene decreases because the value of the total solubility parameter decreases. Then, the polar and hydrogen bonding component of M α CA- α MSt would decrease as compared with M α CA-St. Since the effects of the substitution of a chlorine atom in methacrylate and that of a methyl group in styrene cancel each other out, it is fair to say that the solubility parameter of the ZEP polymer is close to that of P(MMA-St). Consequently, we use the value of P(MMA-St) in place of that of the ZEP polymer.

The distance Ra between a homologous series of *n*-alkyl acetate and polymers are shown in Table II. The distance Ra between these acetates and PMMA, Ra(PMMA), decreases as the size of alkyl group increases; on the other hand, Ra(PSt) is almost constant regardless of the ester size. As a result, Ra(P(MMA-St)) depends on the ester size as a whole, reflecting the dependence of Ra(PMMA), but the dependence is very small. This means that the compatibility between P(MMA-St), or the ZEP polymer, and acetates becomes slightly higher with decreasing ester size.

So, we consider the relationship between the compatibility and the dissolution rate. The compatibility, Ra[P(MMA-St)], does not change rapidly around ethyl-acetate, although the dissolution rate decreases with increasing ester size, especially showing a sharp drop around ethyl-acetate, as shown in Fig. 1(b). This suggests that the dependence of the dissolution rate on various alkyl-acetates cannot be explained merely from the viewpoint of thermodynamic compatibility.

Second, we consider the penetrability of a developer solvent into a polymer matrix. The penetrability strongly depends both on the size of void regions in the polymer matrix, namely, the size of free-volume hole, and on the size of solvent molecules. The dissolution rate decreases as the molecular weight of the solvent increases and hence as solvent molecules become larger. The relationship between the size of solvent molecules and that of void regions is the key to understanding the dissolution phenomena.

For an estimation of the size of a solvent molecule, we used the volume occupied by a molecule, called the van der Waals (VDW) volume. The VDW volume was calculated by

TABLE III. Calculated VDW volumes of a homologous series of *n*-alkyl acetate and methyl ester group.

Component	VDW volume ^{a,b} \AA^3
Methyl-acetate	74.4
Ethyl-acetate	91.4
Propyl-acetate	108.3
Butyl-acetate	125.3
Amyl-acetate	142.2
Hexyl-acetate	159.2
CH ₃ OCO-	55.5

^aVDW radii used for calculations:²⁹ C(1.70 \AA), H(1.20 \AA), and O(1.52 \AA).

^bCovalent bond length used for calculations: C-C(1.54 \AA), C=C(1.34 \AA), C-H(1.10 \AA), C-O(1.43 \AA), and C=O(1.23 \AA).

Bondi's method,²⁹ based on the atomic hard-sphere model. In this calculation, only the overlapped volume between the first nearest neighbor atoms was taken into account. However, it has been reported that this simple method can calculate the VDW volume within an error of 10%, although the calculation depends on the VDW radii, bond distances, bond angles, and molecular geometry used.³⁰ The calculated VDW volumes of a homologous series of *n*-alkyl acetate are summarized in Table III.

For an estimation of the size of void regions, the reported values of polymers resembling ZEP520 were used because the size of voids regions in ZEP resist polymer itself is unknown. The sizes of the void regions in PMMA³¹ and PSt³² have been measured by positron annihilation lifetime spectroscopy. Table IV shows the reported values of the mean radius, mean volume, and volume distribution of the void regions in PMMA and PSt at room temperature. The mean volume of voids is around 80 \AA^3 for PMMA and 110 \AA^3 for PSt. Roughly speaking, the mean volume of the voids in the ZEP polymer, whose monomer unit is close to that of both polymers, is at least between 80 and 110 \AA^3 .

Based on the above estimation, the dependence of the dissolution rate on solvent molecular size is discussed for an unexposed region first. As clearly shown in Fig. 1, there is a critical molecular size of solvent molecules at which the dissolution rate changes dramatically. The reason why there is a critical size can be explained by the relationship between the size of the solvent molecules and the size of voids. The critical size for unexposed films is about the same size as ethyl acetate. Therefore, as shown in Table IV, the critical size is about 90 \AA^3 , which is in the expected range of the mean size

TABLE IV. Reported values of the mean radius, mean volume, and volume distribution of the void regions in polymers at room temperature.

Polymer	M_w	M_w/M_n	Radius R (\AA)	Volume V (\AA^3)	Distribution V (\AA^3)
PMMA ^a	772,600	3.0	2.70	82.4	45–115
PSt ^b	17,500	1.21	2.92	104	70–150
	479,300	1.25	2.95	108	70–150

^aSee Ref. 31.

^bSee Ref. 32.

TABLE V. Effect of developer size and exposure dose on the dissolution process and surface roughness.

Developer	Methyl	Ethyl	Propyl	Butyl	Amyl	Hexyl	Octyl
Molecular size	small		—		large		
Exposure dose	high		—		low		
Size of voids	large		—		small		
Penetrability into aggregates	easy		intermediate		difficult		
Dissolution process	molecular-level		intermediate		aggregate extraction		
Surface roughness	small		large		large		

of voids in the ZEP polymer. Therefore, solvent molecules, such as methyl- and ethyl-acetate, not larger than the critical molecular size could easily penetrate the film through the voids near the surface. As long as solvent molecules are smaller than the voids, the dissolution rate increases with decreasing molecular size. Therefore, the dissolution rate for methyl-acetate is higher than that for ethyl-acetate. On the other hand, molecules larger than the critical molecular size, such as butyl-acetate, could hardly penetrate the film. So, the dissolution is strongly suppressed and the dissolution rate drops rapidly as solvent molecules become larger. Therefore, the bending point appears in the dependence of the dissolution rate on solvent molecules. Studies on the dissolution of poly(methylmethacrylate) (PMMA) film in alkyl-acetate have also found that propyl-acetate has the critical molecular size.^{26–28} These results are exactly alike in that there is a critical molecular size in the dependence of the dissolution rate on the solvent molecular size. It is clear that the limiting step of dissolution of unexposed films is not thermodynamic compatibility but penetrability of solvent molecules into the ZEP resist film.

Next, the dependence of the dissolution rate for an exposed region is discussed. The ZEP polymer is a chain-scission-type resist, whose imaging mechanism is about the same as that of PMMA. Electron-beam exposure fragments the main chain of a polymer as a result of Norrish type I α -cleavage of the ester side chain and the subsequent β -scission reaction. During fragmentation, volatile matter (CO, CO₂, CH₃, etc.) evaporates from the resist film³³ and then voids are formed. Therefore, the electron-beam exposure leads to an increase in the total number of void regions. The size of voids formed after evaporation of the volatile matter is not less than the size of the ester side chain (CH₃OCO-), whose VDW volume is about 60 Å³. Although this is smaller than the critical molecular size, the voids coalesce to form larger voids as the exposure dose increases. Therefore, larger solvent molecules can penetrate the exposed regions. This is why the critical molecular size increases with increasing doses, as shown in Fig. 1.

B. Surface roughness

The generation of surface roughness can be explained by the relationship between the size of developer solvent molecules and the size of the void regions. As mentioned above, the dissolution rate of the exposed resist film strongly de-

pends on this relationship. This characteristic will hold even at the nanometer scale. If the size of the void regions varies from place to place at the nanometer scale, the dissolution rate could also be different from place to place. Therefore, the exposed region does not dissolve uniformly and then surface roughness is generated. As to why the size of void regions varies, we have already focused on polymer aggregates and proposed the aggregate extraction development model. This model is based on the difference in dissolution rate between polymer aggregates and the regions surrounding them, which is due to the difference between the size of voids in the aggregates and those in surrounding regions. It is expected that the size of void regions in the aggregates would distribute mainly in the smaller part of the volume distribution of void regions shown in Table IV, whereas the size of void regions in surrounding regions would distribute in the larger part. This model provides a reasonable explanation of the dependence of the surface roughness on solvent molecular size.

As shown in Fig. 2, small solvent molecules, such as methyl- and ethyl-acetate prevent aggregate extraction development. That is, since these two acetates are small enough to easily penetrate deeply into aggregates, it can dissolve them. As a result, hardly any aggregate extraction development occurs, and the surface roughness is small. This indicates that dissolution proceeds at the molecular level. On the other hand, since large developer molecules from amyl-acetate to octyl-acetates are too large to penetrate aggregates, aggregate extraction development occurs and the surface becomes rough. This explanation means that the dissolution process changes from molecular-level dissolution to aggregate extraction as developer molecules become larger and also that the generation of roughness is deeply related to the dissolution process (Table V).

The situation for propyl- and butyl-acetate is somewhere in between. The size of these two acetate molecules is comparable to the mean size of voids inside aggregates. Therefore, surface morphology no longer shows only the shape of the aggregates. Since the voids have a size distribution in the polymer matrix, these acetates can easily penetrate regions with voids that are larger than these acetate molecules, whereas they cannot readily penetrate those with smaller voids. As a result, dissolution occurs in some regions but not in others. This would explain the appearance of the large undulation on the surface.

Finally, we discuss the dependence of surface morphology on exposure dose. As shown in Fig. 3, the number of the

aggregates or undulations appearing on the surface decreases with increasing dose. This behavior can be similarly explained from the viewpoint of the relationship between the size of solvent molecules and that of voids. Void formation by electron-beam exposure naturally occurs even inside the aggregates. With increasing dose, even large solvent molecules like amyl-acetate can penetrate deeply into the aggregates and dissolve them. The aggregate extraction development is therefore prevented and the number of the aggregates decreases. Similarly, the number of large undulations decreases as the exposure dose increases, as shown in Fig. 3, because of the enlargement of voids inside the undulations. For much larger molecules like octyl-acetate, much higher exposure doses are needed in order for enough voids to be made for the dissolution of the aggregate itself. Therefore, the number of the aggregates hardly decreases. Actually, surface roughness increases with increasing dose for octyl-acetate, as shown in Fig. 4.

V. CONCLUSION

We have clarified the mechanism by which surface roughness is generated by considering the relationship between the size of developer solvent molecules and the size of voids inhomogeneously distributed in the polymer matrix due to polymer aggregates. The magnitude of the surface roughness strongly depends on the size of developer molecules and the exposure dose. Even if a resist film contains aggregates where there are smaller voids than the surrounding regions, solvent molecules smaller than the voids easily penetrate both the aggregates and their surroundings and then dissolve the film uniformly, resulting in less roughness. On the contrary, since a solvent molecule larger than the voids cannot penetrate the aggregates, aggregate extraction occurs, resulting in more roughness. As the exposure dose increases, the voids in the aggregates becomes larger, which makes aggregates themselves easier to dissolve, thus reducing surface roughness. These results indicate that it is very important to understand the relationship between the size of voids during exposure and development and the size of developer molecules to suppress aggregate extraction development and thereby reduce surface roughness of the dissolution front. We were unable to find a developer solvent that satisfies the needs for both high contrast and small roughness at the same time in this study. However, we believe that the control of the size, number, and spatial distribution of void regions in resist films and the selection of an optimum developer solvent is a promising way to reduce line-edge roughness.

ACKNOWLEDGMENTS

The authors would like to thank Junzo Hayashi and Kenji Yamazaki for the electron-beam exposure experiments, and

Kazuhito Inokuma and Dr. Masao Nagase for the AFM observations.

- ¹T. Yoshimura, H. Shiraiishi, J. Yamamoto, and S. Okazaki, *Appl. Phys. Lett.* **63**, 764 (1993).
- ²S. C. Palmateer, S. G. Cann, J. E. Curtin, S. P. Doran, L. M. Eriksen, A. R. Forte, R. R. Kunz, T. M. Lyszczarz, M. B. Stern, and C. Nelson, *Proc. SPIE* **3333**, 634 (1998).
- ³W. Hinsberg, F. A. Houle, J. Hoffnagle, M. Sanchez, G. Wallraff, M. Morrison, and S. Frank, *J. Vac. Sci. Technol. B* **16**, 3689 (1998).
- ⁴M. I. Sanchez, W. D. Hinsberg, F. A. Houle, J. A. Hoffnagle, H. Ito, and C. Nguyen, *Proc. SPIE* **3678**, 160 (1999).
- ⁵G. W. Reynolds and J. W. Taylor, *Proc. SPIE* **3678**, 573 (1999).
- ⁶M. Yoshizawa and S. Moriya, *J. Vac. Sci. Technol. B* **18**, 3105 (2000).
- ⁷H. P. Koh, Q. Y. Lin, X. Hu, and L. Chan, *Proc. SPIE* **3999**, 240 (2000).
- ⁸J. Shin, G. Han, Y. Ma, K. Moloni, and F. Cerrina, *J. Vac. Sci. Technol. B* **19**, 2890 (2001).
- ⁹A. R. Neureuther and C. G. Willson, *J. Vac. Sci. Technol. B* **6**, 167 (1988).
- ¹⁰N. Rau, F. Stratton, C. Fields, T. Ogawa, A. Neureuther, R. Kubena, and C. G. Willson, *J. Vac. Sci. Technol. B* **16**, 3784 (1998).
- ¹¹G. W. Reynolds, J. W. Taylor, and C. J. Brooks, *J. Vac. Sci. Technol. B* **17**, 3420 (1999).
- ¹²T. Yoshimura, H. Shraishi, J. Yamamoto, and S. Okazaki, *Jpn. J. Appl. Phys., Part 1* **32**, 6065 (1993).
- ¹³E. W. Scheckler, S. Shoji, and E. Takeda, *Jpn. J. Appl. Phys., Part 1* **32**, 327 (1993).
- ¹⁴M. Nagase, H. Namatsu, K. Kurihara, K. Murase, and T. Makino, *Microelectron. Eng.* **30**, 419 (1996).
- ¹⁵T. Yamaguchi, H. Namatsu, M. Nagase, K. Yamazaki, and K. Kurihara, *Appl. Phys. Lett.* **71**, 2388 (1997).
- ¹⁶H. Namatsu, Y. Takahashi, K. Yamazaki, T. Yamazaki, M. Nagase, and K. Kurihara, *J. Vac. Sci. Technol. B* **16**, 69 (1998).
- ¹⁷H. Namatsu, T. Yamaguchi, M. Nagase, K. Yamazaki, and K. Kurihara, *Microelectron. Eng.* **41/42**, 331 (1998).
- ¹⁸T. Yamaguchi, H. Namatsu, M. Nagase, K. Yamazaki, and K. Kurihara, *Proc. SPIE* **3333**, 830 (1998).
- ¹⁹H. Namatsu, M. Nagase, T. Yamaguchi, K. Yamazaki, and K. Kurihara, *J. Vac. Sci. Technol. B* **16**, 3315 (1998).
- ²⁰T. Yamaguchi, H. Namatsu, M. Nagase, and K. Kurihara, *Proc. SPIE* **3678**, 617 (1999).
- ²¹C. M. Hansen, *Hansen Solubility Parameters: A User's Handbook* (CRC, Washington, D.C., 1999).
- ²²G. H. Bernstein, D. A. Hill, and W. P. Liu, *J. Appl. Phys.* **71**, 4066 (1992).
- ²³T. Nishida, M. Notomi, R. Iga, and T. Tamamura, *Jpn. J. Appl. Phys., Part 1* **31**, 4508 (1992).
- ²⁴H. Namatsu, M. Nagase, K. Kurihara, K. Iwadate, T. Fukuda, and K. Murase, *J. Vac. Sci. Technol. B* **13**, 1473 (1995).
- ²⁵J. Grank and G. S. Park, *Diffusion in Polymers* (Academic, London, 1968).
- ²⁶E. Gipstein, A. C. Ouano, D. E. Johnson, and O. U. Need III, *Polym. Eng. Sci.* **17**, 396 (1977).
- ²⁷E. Gipstein, A. C. Ouano, D. E. Johnson, and O. U. Need III, *IBM J. Res. Dev.* **21**, 143 (1977).
- ²⁸A. C. Ouano, *Polym. Eng. Sci.* **18**, 306 (1978).
- ²⁹A. Bondi, *J. Phys. Chem.* **68**, 441 (1964).
- ³⁰A. Gavezzotti, *J. Am. Chem. Soc.* **109**, 7968 (1987).
- ³¹K. Süvegh, M. Klapper, A. Domján, S. Mullins, W. Wunderlich, and A. Vértés, *Macromolecules* **32**, 1147 (1999).
- ³²R. M. Dammert, S. L. Maunu, F. H. J. Maurer, I. M. Neelov, S. Niemelä, F. Sundholm, and C. Wästlund, *Macromolecules* **32**, 1930 (1999).
- ³³H. Hiraoka, *IBM J. Res. Dev.* **12**, 121 (1977).